

*Dedicated to Professor Valentin I. Vlad's 70<sup>th</sup> Anniversary*

## ELECTRON COLLISIONS WITH Fe-PEAK ELEMENT Co IV: A COMPUTATIONAL GRAND CHALLENGE

V. STANCALIE

National Institute for Laser, Plasma and Radiation Physics, Department of Lasers, Atomistilor 409,  
P.O. BOX MG-36, Magurele-Ilfov, 077125 Romania, Association EURATOM MEdC,  
E-mail: viorica.stancalie@inflpr.ro

*Received May 20, 2013*

*Abstract.* This paper discusses results from the calculation of electron collision with iron peak element Co IV. It commences with a brief overview of the *R*-matrix method and the calculation performed in LS-coupling. The grand challenge represented by the calculation of accurate atomic data for this ion is then described. Two independent relativistic structure calculations have been performed. Results from the Breit-Pauli and the Dirac-Atomic-*R*-matrix calculations are analyzed comparatively. Discrepancies in energies are noted with the NIST listings for many levels. The implication of these calculations are discussed and finally some future direction of research are reviewed.

*Key words:* electron-ion collision, collision strengths, atomic data calculation.

### 1. INTRODUCTION

Electron impact collision strengths for the low ionization stages of Fe-peak elements Ni and Co and other open d-shell ions are of crucial importance in the quantitative analysis of many laboratory and astronomical spectra. For example, electron impact excited lines in Fe II occur in gaseous nebulae, active galactic nuclei, quasars, Seyfert galaxies, supernovae and the Sun. The deviation of abundances from Fe-peak elements is sensitive to departures from LTE (effects such as over-ionization and resonance scattering). The electron-impact collision strengths for these elements are also important in the analysis of laser-plasma interactions, where transitions in Ni-like ions excited by electron impact are being studied as the basis for efficient X-ray lasers. The accurate theoretical treatment leads to scattering problem involving hundreds of target states and many hundreds, or even thousands, of coupled channels. The complexity of the resonance structure for low-energy electron collisions with such targets requires relativistic effects to be included.

Accurate determination of atomic data for the Fe-peak elements is complicated by the presence of an open 3d-shell in the description of the target ion. The needed atomic data can be obtained in various approximations that differ in

their demands on resources by several orders of magnitude. Ranges of validity of expansions and applicability of perturbation treatments must be established in order to obtain reliable data with the most economical methods. The literature shows how the  $R$ -matrix method is used in atomic collisions. The recent volume by Burke [1] provides both a general review of the  $R$ -matrix method as applied to atomic and molecular collision processes and a very extensive bibliography. The  $R$ -matrix treatments [2-9] have provided results for electron collision with most of the ions of Fe, Ni and Co such as: Fe I, Fe II, Fe III, Fe IV, Fe V, Fe VI, Fe VII, Co V, Co VI, Co II, Ni II, Ni III, Ni V, Ni VI and Ni VII. Apart from our recent work [10] there is no other  $R$ -matrix calculation on Co IV ion.

In the absence of experimental data the need for accurate collision data can be accomplished only through detailed and accurate target description and atomic level energy data calculation. The calculation reported here is part of a general investigation which started with studies of collision strengths for the electron-impact excitation of forbidden transitions between 136 terms arising from  $3d^6$ ,  $3d^54s$  and  $3d^54p$  configurations of  $Co^{3+}$  [10] (hereafter referred to as Paper I and equation x of Paper I will be referred to as (Paper I: x)). In particular, for Co IV ion,  $1s^22s^22p^63s^23p^63d^6\ ^5D$  ground configuration, the energies of the  $3d^54p$  terms are lying between  $3d^6$  and  $3d^54s$  states but overlapping both. Therefore, in Paper I the accuracy of a series of models for the target terms was considered which form the basis of the  $R$ -matrix collision calculations. It was found that one could obtain a better representation for the 136 Co IV levels arising from the  $3d^6$ ,  $3d^54s$ , and  $3d^54p$  manifolds by allowing double electron promotions from the 3p-shell into the 3d-shell and single electron promotion into the 4s and 4p-shell.

In this precursory work collision strengths for the electron impact excitation with  $Co^{3+}$  were calculated for an initial energy range up to 6 Ryd. A number of systematic checks on  $Co^{3+}$  have been performed, exploring the relevance of including configuration interaction wave functions in the target-state expansion and in the  $(N+1)$ -electron quadratically integrable function expansion. The results have shown that when retaining the 136  $LS$ -coupled states, the states formed by the first three configurations overlap each other in energy but the  $3d^44s^2$  states all lie higher. However, the  $3d^44s^2$ ,  $3d^44s4p$  and  $3p^53d^7$  levels overlap each other. In order to explore the effect of including of additional states, we have performed additional collision calculation including a further 136 states which arise from the inclusion of the fourth  $3d^54d$  configuration in the  $R$ -matrix expansion. Results are presented in Section 2. The size of the actual collision problem doubles to 272 coupled states yielding on the order of 2000 coupled channels. The key conclusion of these preliminary investigations, which have been performed in  $LS$  coupling, is that the interaction between the lowest even configurations and the perturbation on odd parity configurations play an important role in such calculations. Therefore, we have decided to study the relativistic effects. Section 3 presents results from the semi-relativistic *Breit-Pauli*  $R$ -matrix (BPRM) calculation. In our BPRM calculations [11] (hereafter referred to as Paper II and equation x of Paper II will be referred to as (Paper II: x)), we have constructed an eigenfunction expansion over

the three configurations  $3d^6$ ,  $3d^5 4s$ , and  $3d^5 4p$  of  $\text{Co}^{3+}$ , yielding 136 fine-structure levels corresponding to 43  $LS$  terms. At this level of accuracy we have compared the theoretical data with the available experimental data in Atomic Structure Database (ASD) of the National Institute for Standards and Technology (<http://www.nist.gov>). The ASD data is based on the compilation of Co ions by Sugar and Corliss in [12]. In their work, all energy levels are given in units of  $\text{cm}^{-1}$ , beginning with a value of zero for the ground levels. Although uncertainties are not provided with these extrapolated values, the levels uncertainty is presumed  $\pm 0.5\text{cm}^{-1}$ . In Section 4 full relativistic calculation results are presented. The energies, lifetimes, and wave-function contributions have been computed for all levels of a six target set configuration allowing for single excitation into the 4s and 4p shell and double electron excitation from 3p-shell into the 3d-shell. We have used the General-purpose Relativistic Atomic Structure Package (GRASP)[13]. Additionally, two similar full relativistic calculations have been performed for two sets of three and four non-relativistic configurations, which include all levels arising from  $3d^6$ ,  $3d^5 4s$  and  $3d^5 4p$ , and  $3d^6$ ,  $3d^5 4s$ ,  $3d^5 4p$ ,  $3p^5 3d^7$  configurations, respectively. By comparing the levels energy calculated by these three different target set configurations, we carefully assess the accuracy of our theoretical results. Section 5 gives our concluding remarks and the future directions of research.

## 2. PERTURBATIVE CALCULATION

In Paper I we have initiated a study of electron impact excitation of  $\text{Co}^{3+}$ ,  $1s^2 2s^2 2p^6 3s^2 3p^6 3d^6$  ( $^5D^e$ ) ground configuration, considering the forbidden transitions which arise between the 136 terms of the  $3d^6$ ,  $3d^5 4s$  and  $3d^5 4p$  configurations. The computer programs which have been used in our  $R$ -matrix electron-ion collision calculations correspond to (i) target state calculation; (ii) internal region calculation yielding the  $R$ -matrix on the boundary  $r = a$ ; (iii) external and asymptotic region calculation yielding the  $K$ -matrix,  $S$ -matrix and collision cross sections. In the first stage of the calculation we used CIV3 program [14] to obtain accurate target state energies and wave functions (Paper I: 1) which are used in the following stages of the  $R$ -matrix calculations. In the second stage of calculation we used RMATRXI program [15] to solve the electron-atom collision problem in the  $R$ -matrix internal region. In the third stage of calculation we used FARM, written by Burke and Noble [16] to solve the electron-atom collision problem in the  $R$ -matrix external and asymptotic regions. These programs enable the  $K$ -matrix,  $S$ -matrix and hence collision strengths to be determined. The target wave functions and the  $(N+1)$ -electron quadratically integrable functions employed in the Equation Paper I:1 are constructed with a common set of one-electron spin-orbital functions. In the asymptotic region, the radius is propagated to a new distance, chosen large enough that the radial functions which represent the colliding electron can be accurately represented by an asymptotic expansion. The

K-matrix elements and the S-matrix elements, and therefore the collision strengths  $\Omega_{ij}$  can be easily calculated by matching the solution of the inner and outer regions at the R-matrix boundary radius  $r = a$ . For completeness the expression for the electron scattering cross section is given herein. The expressions for the S-matrix and T-matrix as related to the K-matrix are:

$$S = (1 + iK)(1 - iK)^{-1} \quad T = S - 1, \quad (1)$$

where these matrices have particular total  $J$  and  $\pi$  values. The partial collision strength which contributes to the cross section for a transition of the target from state  $r$  to a state  $s$  is a summation over the channels  $\alpha_r J_r^t j_r$  to  $\alpha_s J_s^t j_s$  that are coupled to them.  $\alpha$  represents all the other quantum numbers that uniquely identify a target state. The total collision strength is a sum of the partial collision strengths for each symmetry:

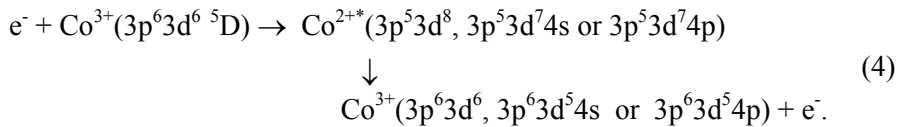
$$\Omega_{rs}^{J\pi} = \frac{g}{2} \sum_{j_r j_s} |T_{rs}|^2, \quad \Omega_{rs} = \sum_{J\pi} \Omega_{rs}^{J\pi}, \quad (2)$$

where  $g = 2J + 1$ , for  $jj$  coupling and  $\Omega_{rs}$  should be symmetric. Then the total cross section for this transition is given by

$$\sigma_{r \rightarrow s} = \frac{\pi a_0^2}{k_r^2 g_r} \Omega_{rs}, \quad (3)$$

where  $g_r = 2J_r^t + 1$  and  $a_0$  is the Bohr radius to convert from atomic units.

The following excitation ways (Paper I:3) have been included in our study:



In this earlier work, three target-model calculation have been developed: a) a *three LS-coupled R-matrix* calculation (Calculation A) including  $3d^6$ ,  $3d^5 4s$  and  $3d^5 4p$  states in the  $N$ -electron wave-function expansion; b) a *six target-model* calculation (Calculation B), where electron correlation effects were explored by carrying out separate calculations with six configurations  $3d^6$ ,  $3d^5 4s$ ,  $3d^5 4p$ ,  $3p^4 3d^8$ ,  $3p^4 3d^7 4s$  and  $3p^4 3d^7 4p$  in the target state expansion and the configurations  $3d^7$ ,  $3d^6 4s$ ,  $3d^6 4p$ ,  $3d^5 4s^2$ ,  $3d^5 4s 4p$ ,  $3d^5 4p^2$ ,  $3p^5 3d^8$ ,  $3p^4 3d^9$ ,  $3p^5 3d^8$ ,  $3p^4 3d^9$ ,  $3p^4 3d^8 4s$  and  $3p^6 3d^5 4s^2$  in the  $(N+1)$ -electron quadratically integrable function expansion; and c) a *nine target-model* calculation (Calculation C). Starting with the 136-level model, we have included in the R-matrix expansion all 184 *LS* coupled states which arise from nine target configuration  $3d^6$ ,  $3d^5 4s$ ,  $3d^5 4p$ ,  $3p^4 3d^8$ ,  $3p^4 3d^7 4s$ ,  $3p^4 3d^7 4p$ ,  $3p^5 3d^7$ ,

$3p^5 3d^6 4s$  and  $3p^5 3d^6 4p$ . The 136  $LS$  target states arising from the *three, six and nine* basis configurations above, were optimally represented by configuration interaction type expansions in terms of eight orthogonal basis orbitals.

For collision calculations, a number of systematic checks on  $\text{Co}^{3+}$  have been performed. We have investigated the position of  $3d^5 4d$  and  $3d^4 4s^2$  terms including the configurations  $3d^5 4s^2$ ,  $3d^5 4p^2$ ,  $3d^5 4d^2$ ,  $3d^5 4s 4p$ ,  $3d^5 4p 4d$  in the  $(N+1)$ -electron quadratically integrable function expansion. The  $3d^5 4d$  terms are lying between  $3d^5 4p$  and  $3d^4 4s^2$  states but overlapping both. To illustrate the complexity of this problem, in Paper II we have decided to carry out a first calculation in which 272  $LS$  terms of the four configurations  $3d^6$ ,  $3d^5 4s$ ,  $3d^5 4p$  and  $3d^5 4d$  with a maximum 841 channels which includes the  $3p^6 3d^5 4d$  configuration, are included in the  $R$ -matrix expansion. Figure 1 presents a comparison between the collision strengths as outputs from two different calculations where 136 terms (Paper I) arising from the  $3d^6$ ,  $3d^5 4s$ ,  $3d^5 4p$  manifolds, and 272 terms (Paper II) arising from  $3d^6$ ,  $3d^5 4s$ ,  $3d^5 4p$  and  $3d^5 4d$  manifolds are included into the  $R$ -matrix expansion, respectively. The inclusion of additional states affects the resonance structure in the collision strengths. The collision strength results correspond to the transition from the ground state  $3d^6$  ( $^5D^e$ ) to the first excited state  $3d^6$  ( $^3P^e$ ),  $^4F^e$  symmetry. As shown in Figure 1 the resonance positions are pushed to lower scattered electron energies.

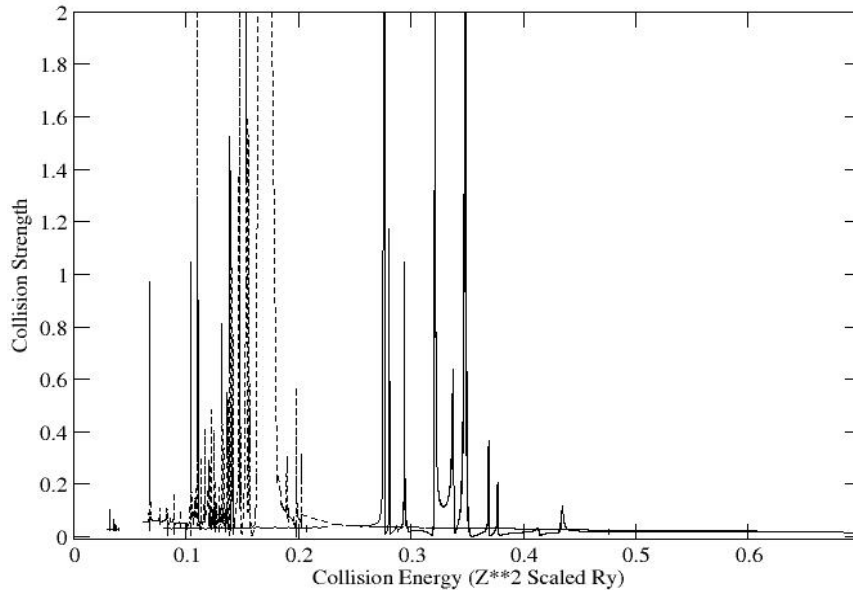


Fig.1 – Collision strength for the  $^5D^e - ^3P^e$  transition of  $\text{Co}^{3+}$ . The full curve corresponds to the first calculation (Paper I) where the only  $3d^6$ ,  $3d^5 4s$  and  $3d^5 4p$  target states are included into the  $R$ -matrix expansion. The broken curve corresponds to Paper II work where the  $3d^6$ ,  $3d^5 4s$ ,  $3d^5 4p$  and  $3d^5 4d$  target states are included into the  $R$ -matrix expansion. Scaled units are used for collision energy: for positively charged ions energies are scaled by a factor  $1/Z^2$ , with  $Z = 3$  for  $\text{Co}^{3+}$  ion.

The obtained results from above analysis have determined the initiation of the nine configurations LS-coupled  $R$ -matrix calculation. This largest calculation shows the effect on the collision strengths of including additional 48 levels with electronic configuration  $3p^53d^7$ . In this calculation the target states were represented by nine configurations  $3d^6$ ,  $3d^54s$ ,  $3d^54p$ ,  $3p^43d^8$ ,  $3p^43d^74s$  and  $3p^43d^74p$ ,  $3p^53d^7$ ,  $3d^44s^2$  and  $3d^44s4p$ , and correspondingly the  $(N+1)$ -electron configurations  $3p^63d^7$ ,  $3p^63d^64s$ ,  $3p^63d^64p$ ,  $3p^63d^64s^2$ ,  $3p^63d^54s4p$ ,  $3p^63d^54p^2$ ,  $3p^53d^8$ ,  $3p^43d^9$ ,  $3p^43d^84p$ ,  $3p^43d^74s4p$ ,  $3p^53d^74p$ ,  $3p^43d^74p^2$ ,  $3p^53d^64s^2$ ,  $3p^53d^64s4p$  and  $3p^53d^64p^2$ . In figure 2 we present graph of the collision strengths against incident electron energy for the third calculation and the same transition plotted in Fig. 1.

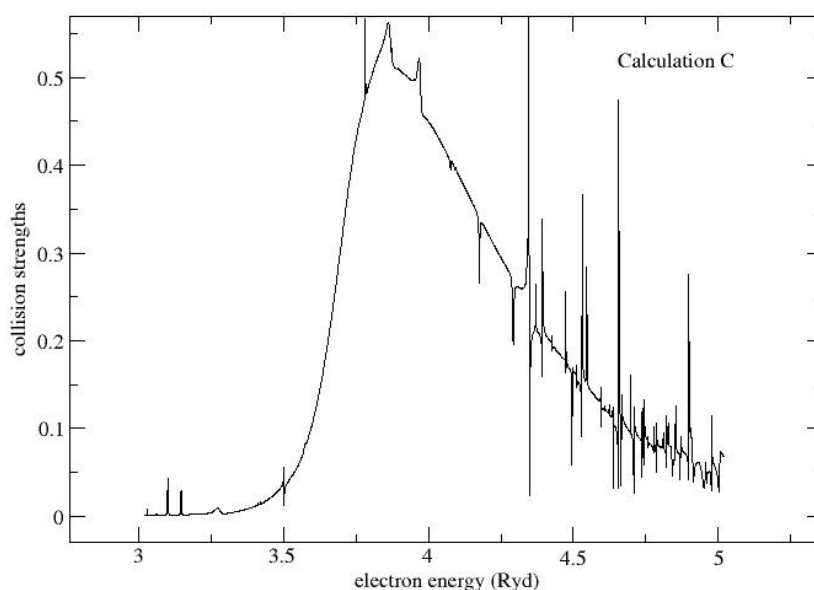


Fig. 2 – Collision strength for the  ${}^5D^e - {}^3P^e$  transition of  $Co^{3+}$ . The curve corresponds to the third calculation: Calculation C. In this calculation nine target state configurations  $3d^6$ ,  $3d^54s$ ,  $3d^54p$ ,  $3p^43d^8$ ,  $3p^43d^74s$ ,  $3p^43d^74p$ ,  $3p^53d^7$ ,  $3d^44s^2$  and  $3d^44s4p$  are included into the  $R$ -matrix expansion.

This figure shows new Rydberg series of resonances associated with  $3p^53d^7$  states. It is found that the inclusion of additional the 48 states associated with  $3p^53d^7$  state yields to additional resonance structures while the resonance structure observed in figure 1 is moved down in energy, very slightly.

### 3. SEMI-RELATIVISTIC BREIT-PAULI R-MATRIX CALCULATION

The Breit-Pauli R-matrix (BPRM) method includes relativistic effects in the Breit-Pauli approximation. It enables the calculations of both the dipole allowed

( $\Delta S = 0$ ) and the intercombination ( $\Delta S \neq 0$ ) transitions, in contrast to *LS* calculations where only the dipole allowed transitions can be included. Incorporation of the relativistic effects in the close coupling R-matrix method yields a large number of fine structure transition probabilities with higher accuracy. The fine structure energy levels are obtained as the eigenvalues of the Breit-Pauli Hamiltonian labeled by the total angular momentum and parity, i.e.  $J\pi$ .

The Hamiltonian is written as follows (Paper II: 5):

$$H_{N+1}^{BP} = H_{N+1}^{NR} + H_{N+1}^{mass} + H_{N+1}^{DAR} + H_{N+1}^{so}, \quad (5)$$

where  $H_{N+1}^{NR}$  is the nonrelativistic Hamiltonian,  $H_{N+1}^{mass}$  is the one-body mass-velocity term,  $H_{N+1}^{DAR}$  is the Darwin term, and  $H_{N+1}^{so}$  is the spin-orbit term. This last term breaks *LS* symmetry leading to fine-structure levels  $J\pi$  of total angular momentum quantum number  $J$  at parity  $\pi$ . In relativistic BPRM calculations, sets of collisional symmetry  $SL\pi$  are recoupled to obtain the states of the ( $N+1$ ) atomic system with total  $J\pi$ , followed by diagonalization of the ( $N+1$ )-electron Hamiltonian. Details of diagonalizing  $H_{N+1}^{BP}$  at the  $R$ -matrix boundary are given in [15] as is the outward propagation. In Paper II, an initial semi-relativistic *Breit-Pauli*  $R$ -matrix calculation has been done. We have constructed an eigenfunction expansion over the three configurations  $3d^6$ ,  $3d^54s$ , and  $3d^54p$  of  $\text{Co}^{3+}$ , yielding 136 fine-structure levels corresponding to 43 *LS* terms. Eight orthogonal one-electron orbitals  $1s$ ,  $2s$ ,  $2p$ ,  $3s$ ,  $3p$ ,  $3d$ ,  $4s$  and  $4p$  were used both in the definition of the target states and also for the ( $N+1$ )-electron quadratically integrable functions. The calculation considers all possible bound levels for  $0 \leq J \leq 8$  with  $0 \leq L \leq 7$ , and  $(2S+1) = 1, 3, 5, 7$  even and odd parities. The intermediate coupling calculations are carried out on recoupling the *LS* symmetries in a pair-coupling representation. The (electron + core) Hamiltonian matrix is diagonalized for each resulting  $J\pi$ . The number of coupled channels was 1024 and the Hamiltonian matrix size was 20 502. Table 1 reproduces selected results for lowest even parity energy levels from the BPRM calculation and comparison with ASD data. The energy difference average percentage of the low-lying levels agrees to within 3.9 % of each other.

Given detailed calculation provided here and comparison with our earlier work (Paper I), we estimate that the accuracy of our data is within 20% for transitions within the  $3d^6$  manifold. Due to the lack of experimental data for electron impact excitation on this complex ion there is no way to fully assess the accuracy of our calculations.

Table I

Comparison between the calculated Breit-Pauli  $R$ -matrix theoretical levels energy and the experimental data from ASD, in Rydberg units: Paper II

<i>index</i>	Configuration	$^{2S+1}L_J$	ASD[Ryd]	Paper II [Ryd]	Diff
1	$3d^6$	$(^5D_4)$	0.0000	0.000000	0.000
2		$(^5D_3)$	0.005824	0.0062954	-0.000471
3		$(^5D_2)$	0.0098207	0.0106945	-0.000874
4		$(^5D_1)$	0.012369	0.0135196	-0.001151
5		$(^5D_0)$	0.013611	0.0149041	-0.001293
6	$3d^6$	$(^3P_2)$	0.208528	0.2625710	-0.054043
7		$(^3P_1)$	0.225349	0.2811257	-0.055776
8		$(^3P_0)$	0.231906	0.2885840	-0.056678
9	$3d^6$	$(^3H_6)$	0.215783	0.2406979	-0.024915
10		$(^3H_5)$	0.218994	0.2438954	-0.024901
11		$(^3H_4)$	0.221183	0.2461911	-0.025008
12	$3d^6$	$(^3F_4)$	0.231425	0.2753618	-0.043937
13		$(^3F_3)$	0.234523	0.2789963	-0.044473
14		$(^3F_2)$	0.236647	0.2817250	-0.045080
15	$3d^6$	$(^3G_5)$	0.264466	0.3040261	-0.039560
16		$(^3G_4)$	0.269664	0.3101048	-0.040441
17		$(^3G_3)$	0.272173	0.3125937	-0.040421
18	$3d^6$	$(^1I_6)$	0.327534	0.3634301	-0.035896
19	$3d^6$	$(^3D_3)$	0.331227	0.3936521	-0.062425
20		$(^3D_3)$	0.333109	0.3954644	-0.062355
21	$3d^6$	$(^1G_4)$	0.334283	0.3842885	-0.050005
22	$3d^6$	$(^1S_0)$	0.377646	0.4465629	-0.068917
23	$3d^6$	$(^1D_2)$	0.385847	0.4774924	-0.091645
24	$3d^6$	$(^1F_3)$	0.461375	0.5506971	-0.089322

#### 4. FULL RELATIVISTIC DIRAC-ATOMIC $R$ -MATRIX CALCULATION

In the present work we report results for fine-structure energy levels, the term splitting, and wave-functions composition calculated with the extended average level multi-configurational Dirac-Fock method (MCDF-EAL) in the general-purpose relativistic atomic structure package (GRASP). We briefly describe the Dirac Hamiltonian approach which has the advantage that all the relativistic effects are included not only for the eigenenergies but, most importantly, in the radial wave-functions. The GRASP code is fully relativistic and is based on the  $jj$  coupling scheme. We have used the extended average level MCDF-EAL option where in the Hamiltonian matrix we minimize a weighted trace (proportional to  $2J+1$ ). Additional relativistic corrections arising from the Breit interaction and quantum electrodynamics (QED) are also included. Energies have been computed for all levels of  $3p^63d^6$ ,  $3p^63d^54s$ ,  $3p^63d^54p$ ,  $3p^43d^8$ ,  $3p^43d^74s$  and  $3p^43d^74p$  allowing double electron promotions from the 3p-shell into the 3d-shell and single

electron promotion into the 4s and 4p-shell to generate expansions for the multiconfiguration Dirac-Hartree-Fock approximation. This type of calculation gives a set of 12 bound orbitals which is optimized over all the levels included. The resulting 12 relativistic orbitals produced 2459  $J\pi$  levels, all of which are to be used in close-coupling expansion. In the MCDF approach, intermediate coupling wave-functions  $\Psi_\gamma(J)$  are constructed by using an expansion of the form [18, 19]:

$$\Psi_\gamma(J) = \sum_\alpha c_\gamma(\alpha J) \Phi(\alpha J), \quad (6)$$

where configuration wavefunctions (CSFs)  $\Phi(\alpha J)$  are expressed as antisymmetrized products of two-component orbitals

$$\phi(r) = \frac{1}{r} \begin{pmatrix} P_{nlj}(r) \chi_{ljm}(\hat{r}) \\ iQ_{nlj}(r) \chi_{ljm}(\hat{r}) \end{pmatrix}. \quad (7)$$

Here  $P_{nlj}$  and  $Q_{nlj}$  are the large and small radial components of one-electron wave-functions and  $\chi_{ljm}(\hat{r})$  are the two component Pauli spherical spinors. Two-component orbitals are obtained as the self-consistent solutions of the Dirac-Fock equations systematically increasing configuration interaction basis. Direct and indirect relativistic effects are included in the relativistic wave-functions by solving MCDF equations. The configuration mixing coefficients,  $c_\gamma$ , are obtained through diagonalization of the Dirac-Coulomb Breit-Hamiltonian:

$$H^{DF} = \sum_i h_i^D + \sum_{i<j} h_{ij}^e + \sum_{i<j} h_{ij}^{trans} \quad (8)$$

Where  $h_i^D$  is one-electron Dirac-Hamiltonian,  $h_{ij}^e$  is the instantaneous Coulomb repulsion. The effects of the transverse interaction  $h_{ij}^{trans}$  that corresponds to the Breit interaction:

$$h_{ij}^{Breit} = -\frac{\alpha_i \cdot \alpha_j}{2r_{ij}} - \frac{(\alpha_i \cdot r_{ij})(\alpha_j \cdot r_{ij})}{2r_{ij}^3} \quad (9)$$

are evaluated in the first order of perturbation expansion. QED corrections, which include vacuum polarization and self-energy (known as the Lamb shift), are considered in the first order of perturbation theory. In our full relativistic calculation the orbital data are defined by six non-relativistic configuration state functions (CSFs) included in the above mentioned  $LS$  six target-model calculation, namely:  $3p^6 3d^6$ ,  $3p^6 3d^5 4s$ ,  $3p^6 3d^5 4p$ ,  $3p^4 3d^8$ ,  $3p^4 3d^7 4s$  and  $3p^4 3d^7 4p$ . The resulting 12 relativistic orbitals produced 2459  $J\pi$  levels, with angular momentum  $0 \leq J \leq 9$ , even and odd parity. More than  $7 \times 10^6$  radiative rates have been calculated. Table 2 lists the lowest levels of  $\text{Co}^{3+}$  as output from the code, along with the leading

percentage composition  $c_\gamma (\alpha J)^2$ . We also give in that table the dominant CSFs that contribute to these levels. The weight given in Table 2 represents the mixing coefficients squared when transformed from  $jj$  to the  $LS$  CSF basis. The resulting  $N$ -electron levels are labeled by total angular momentum  $J$  and parity  $\pi$ . The Atomic Spectra Database (ASD) reports the leading percentage of the wave-function composition from calculation using the Cowan code [20].

Comparing the level composition in Table 2 with ASD data, we note the differences (for example, the ground state is only 99.8 in the present work whereas it accounts for 100% of the wave-function composition in ASD). The possible source that may contribute to these differences is the method of calculation. The present method is an *ab initio* method, while the wave-function composition reported in ASD is a semi-empirical calculation. In the calculation, the Dirac Coulomb contribution is largest, with Breit interaction giving a significant correction. Many levels have switched when Breit is added. Fairly good agreement is obtained for the (MCDF) calculations, the energy difference average percentage of the low-lying levels usually agreeing to within 2 % of each other.

Finally, we mention that preliminary calculation of collision strengths within the Dirac  $R$ -matrix approach has been started. This large calculation is not reported here. As stated above, we first employed the GRASP code to calculate energy levels and A-values for Co IV.

Table 2

Level energies in Co IV in Rydberg units. Experimental values (exp.) are from the NIST Atomic Structure Database (ASD) (<http://www.physics.gov>)

CSF	$J^\pi$	Weight(%)	E(MCDF)	E (exp.)	Diff.
$3d^6$	4+	0.998 $\pm$ 0.0005	0.00	0.000	0.000
$3d^6$	3+	0.998 $\pm$ 0.001	0.004932	0.005824	0.0008
$3d^6$	2+	0.998 $\pm$ 0.001	0.008379	0.0098207	0.0014
$3d^6$	1+	0.997 $\pm$ 0.001	0.010589	0.012369	0.0017
$3d^6$	0+	0.997 $\pm$ 0.001	0.011670	0.013611	0.0019
$3d^6$	2+	0.750 $\pm$ 0.013	0.241685	0.208528	-0.0331
$3d^6$	1+	0.750 $\pm$ 0.001	0.255835	0.225349	-0.0304
$3d^6$	0+	0.750 $\pm$ 0.001	0.261488	0.231906	-0.0295
$3d^6$	6+	0.998 $\pm$ 0.0005	0.268235	0.215783	-0.0524
$3d^6$	5+	0.991 $\pm$ 0.002	0.271144	0.218994	-0.0521
$3d^6$	4+	0.660 $\pm$ 0.011	0.272023	0.2314250	-0.0405
$3d^6$	4+	0.993 $\pm$ 0.004	0.274529	0.221183	-0.0533
$3d^6$	3+	0.866 $\pm$ 0.004	0.276111	0.234523	-0.0415
$3d^6$	2+	0.779 $\pm$ 0.005	0.277962	0.236647	-0.0413
$3d^6$	5+	0.991 $\pm$ 0.002	0.319667	0.264466	-0.0552
$3d^6$	4+	0.984 $\pm$ 0.004	0.323801	0.269664	-0.0541
$3d^6$	3+	0.991 $\pm$ 0.003	0.326200	0.2721721	-0.0540

Table 2 (continued)

$3d^6$	2+	$0.780 \pm 0.014$	0.382426	0.334283	-0.0481
$3d^6$	3+	$0.997 \pm 0.001$	0.391975	0.331537	-0.0604
$3d^6$	2+	$0.992 \pm 0.002$	0.391 862	0.331 227	-0.0607
$3d^6$	3+	$0.996 \pm 0.001$	0.393 615	0.333 109	-0.0602
$3d^6$	6+	$0.998 \pm 0.0005$	0.405 438	0.327 534	-0.0763

## 5. CONCLUDING REMARKS

In the present work we discuss results from three R-matrix approaches which have been used to study the electron collision with iron peak element  $\text{Co}^{3+}$ . They are the non-relativistic, the semi-relativistic Breit-Pauli and the full relativistic Dirac-Fock *R*-matrix methods. The major components of the wave-function have been compared in both *jj* and *LSJ* coupling. Although in *jj* coupling most of the expansions have a dominant component, the *LSJ* label can be used to identify the *LS*-forbidden transitions. We see that for the  ${}^5\text{D}^e - {}^3\text{P}^e$  low-lying transition, the effect of including additional configuration in the *R*-matrix expansion is to modify the resonance structure at low collision energy.

In order to gain an understanding of the grand challenge that present and the future calculation requires, we refer to results already obtained from full relativistic treatment within the Dirac- Atomic *R*-matrix approach. During the calculation, the Breit interaction and QED effects have been included, together with the *extended average level* in which a weighted  $(2j+1)$  trace of Hamiltonian matrix is minimized. This produced a compromised set of orbitals describing closely lying states with moderate accuracy. Comparing results from BPRM and DARC calculation discrepancies in energies are observed with the NIST listings for many levels, particularly those belonging to the  $(3d^5)4s$  and  $4p$  configurations. It soon became clear that the level of configuration interaction (CI) required for Co IV is too large and the desired calculations cannot be performed with the GRASP code within a reasonable time frame of a few months.

The increasing sophistication of collision calculations depends to a considerable extent on rapidly increasing power of the supercomputers available to such research. A number of developments are now underway or are planned. These include a new kind of data representation that allows for parallel computing due to multiple storage servers employed, combined with data storage in binary files. It is an advanced graph database tool for data representation and data processing. The new computation work for Co IV ion is in progress and includes several sets of calculations with varying amount of CI. The increasing configuration interaction with up to 21 configurations generates up to 14732 levels. The new graph representation technique which requires development and implementation of advanced algorithms will enable to run many times faster, optimizing both size and speed of the numerical codes.

**Acknowledgements.** Financial support under the Romanian Space Agency coordinated program STAR Project Number 33 is gratefully acknowledged.

## REFERENCES

1. P. G. Burke, *R-Matrix theory of atomic collision*, Springer Series on Atomic, Optical and plasma Physics, **61**, Springer, Heidelberg, Dordrecht, London, New-York, 2011.
2. S.N. Nahar, *Atomic data from the Iron Project*, Astronomy & Astrophysics, **457**, 721–728 (2006).
3. C.A. Ramsbottom, M.P. Scott, K.L. Bell, F.P. Keenan, B.M. McLaughlin, A.G. Sunderland, V.M. Burke, C.J. Noble, P.G. Burke, *Electron impact excitation of the iron peak element Fe II*, J. Phys. B: At. Mol. Opt. Phys., **35**, 3451–3478 (2002).
4. C.A. Ramsbottom, C.J. Noble, V.M. Burke, M.P. Scott, P.G. Burke, *Configuration interaction effects in low-energy electron collisions with Fe II*, J. Phys. B: At. Mol. Opt. Phys., **37**, 3609–3632 (2004).
5. C. A. Ramsbottom, C. J. Noble, V.M. Burke, M.P. Scott, R. Kisielius, P.G. Burke, *Electron impact excitation of Fe II: Total LS effective collision strengths*, J. Phys. B: At. Mol. Opt. Phys., **38**, 2999–3014 (2005).
6. M.P. Scott, C. A. Ramsbottom, C.J. Noble, V.M. Burke, P.G. Burke, *On the role of ‘two-particle-one-hole’ resonances in electron collisions with Ni V*, J. Phys. B: At. Mol. Opt. Phys., **39**, 387–400 (2006).
7. K.A. Berrington, J.C. Pelan, *Atomic data from the IRON Project XII. Electron excitation of forbidden transitions in V-like ions Mn III, Fe IV, Co V and Ni VI*, Astron. Astrophys. Suppl. Ser., **114**, 367–371 (1995).
8. M.S.T. Watts, V.M. Burke, *Electron impact excitation of complex atoms and ions III: Forbidden transitions in Ni<sup>2+</sup>*, J. Phys. B: At. Mol. Opt. Phys., **31**, 145–156 (1998).
9. M.S.T. Watts, *Electron-impact excitation of complex atoms and ions: V. Forbidden transitions in Co<sup>+</sup>*, J. Phys. B: At. Mol. Opt. Phys., **31**, 2065–2076 (1998).
10. V. Stancalie, *Forbidden transitions in excitation by electron impact in Co<sup>3+</sup>: an R-matrix approach*, Physica Scripta, **83**, 025301 (2011).
11. V. Stancalie, *Complements to the theoretical treatments of the electron collision with Co<sup>3+</sup>: An R-matrix approach*, Journal of Spectroscopy, **1**, 82063 (2013).
12. J. Sugar, Ch. Corliss, *Atomic Energy Levels of the Iron Period Elements: Potassium through Nickel*, J. Phys. Chem. Ref. Data, **14**, Supplement No.2, 279–296 (1985).
13. K. G. Dyall, I. P. Grant, C. T. Johnson, F. A. Parpia, E. P. Plummer, *GRASP: A general-purpose relativistic atomic structure program*, Comput. Phys. Commun., **55**, 425–456 (1989).
14. A. Hibbert, CIV3- *A general program to calculate configuration interaction wave functions and electric-dipole oscillator strengths*, Comput. Phys. Commun., **9**, 141–172, (1975).
15. K.A. Berrington, W.B. Eissner, P.H. Norrington, *RMATRX1: Belfast atomic R-matrix codes*, Comput. Phys. Commun., **92**, 290–420 (1995).
16. V.M. Burke and C.J. Noble, *FARM: Flexible Asymptotic R-Matrix code*, Comput. Phys. Commun., **85**, 471–500 (1995).
17. D.W. Busby, P.G. Burke, V.M. Burke, C.J. Noble, N.S. Scott, I.T.A. Spence, *HBrowse: a GRACE tool for browsing R-matrix H-files*, Computer Physics Communications, **131**, 202–224 (2000).
18. I. Grant, *The Dirac operator on a finite domain and the R-matrix method*, J. Phys. B: At. Mol. Opt. Phys., **41**, 055002 (2008).
19. V. Jonauskas, F. P. Keenan, M. E. Foord, R. F. Heeter, S. J. Rose, G. J. Ferland, R. Kisielius, P.A.M. Hoof, P.H. Norrington, *A&A*, **424**, 363 (2004).
20. R. D. Cowan, *The theory of atomic structure and spectra*, University of California Press, Berkeley, 1981.